# Energy-Efficient Multi-Relaying with NOMA for Sustainable Communication in Smart Environments

**Indrajeet Kumar[1] and S S P M Sharma B[2]**
Associate Professor, Computer Engineering & Information Technology Department, School of Engineering, P P Savani University, Surat, India[1]
Assistant Professor, Mechatronics Engineering, Parul University, Vadodara, Gujarat, India[2]

**Abstract:**
This paper proposes an energy-efficient communication framework tailored for smart and sustainable environments, integrating finite block length (FBL) transmission with non-orthogonal multiple access (NOMA) and hybrid one-way/two-way multi-relaying. The system employs a shared decode-and-forward (DF) relay to facilitate information exchange between two source nodes and their respective destinations, within a constrained number of channel uses—thereby optimizing spectral and energy resources. Closed-form expressions for the end-to-end block error rate (BLER) and net system throughput are derived, providing critical insights into reliability and efficiency. Moreover, an asymptotic BLER floor is established under high signal-to-noise ratio (SNR) conditions. Simulation results confirm the analytical findings and demonstrate the proposed model's potential in reducing energy consumption and enhancing data reliability. This work contributes to the development of sustainable wireless communication systems for next-generation smart networks.

## INTRODUCTION

In order to facilitate machine-to-machine (M2M) communication and the internet of things (IoT), the wireless networks of the fifth generation (5G) are designed to have high spectral efficiency, quick connection, and low latency [1]. Researchers have shown a great amount of interest in cooperative relay-aided non-orthogonal multiple access (NOMA) communication in this respect. As a result of the cooperative nature of the NOMA architecture, multiple users are able to share the same frequency and time resources, which results in an expanded network. Numerous studies have shown that cooperative relay-aided NOMA protocols have a higher spectrum efficiency than orthogonal multiple access (OMA) approaches. This is in contrast to the results of the OMA methods [2]- [5].

Previous studies on non-orthogonal multiple access (NOMA) have predominantly utilized the classical Shannon approach for performance analysis, which relies on very long blocklengths for accurate results [6]. However, such long blocklengths are impractical and unsuitable for the dynamic and bursty communication characteristic of NOMA-based internet of things (IoT) or machine-to-machine (M2M) networks in the 5G era. Therefore, there is a need to shift towards a new analysis paradigm that is better suited for evaluating IoT networks [7]- [9].

Researchers have explored the feasible block error rate (BLER) when employing finite blocklength (FBL) transmissions in order to solve the limitations that come with doing long blocklength analyses in non-orthogonal multiple access (NOMA) systems [10], [11]. In previous research, FBL NOMA systems were investigated in both non-cooperative downlink settings as well as cooperative downlink scenarios facilitated by decode-and-forward (DF) one-way relay communication. Additionally, in an FBL communication system, an investigation into the usage of two-way relays to improve spectral efficiency has been carried out. Nevertheless, there is a hole in the research regarding the performance analysis of joint one-way and two-way relaying systems. These systems have the potential to significantly improve the spectrum efficiency of NOMA when used in conjunction with FBL [12].

Through the use of simultaneous one-way and two-way relaying, this work presents a unique non-orthogonal multiple access (NOMA) scheme and analyses the resulting block error rate (BLER) and throughput [13]. The proposed protocol mimics a two-way relaying system by having two source nodes communicate over a single decode-and-forward (DF) relay. Similar to a one-way relaying system, the relay also helps in the transmission of information symbols from the source nodes to the destination nodes [14]- [18]. This allows for the transmission of four message signals across the channel over the course of two phases using the channel's finite capacity. The suggested system has great potential for use in industrial automation and environment monitoring situations involving IoT sensors/devices or autonomous machines that need to communicate and coordinate information before transmitting it to their respective information processors [19]- [21]. The paper summarises the major findings and explains how they fit together.

In Section II, we offer the paper's system model for the NOMA-based new joint one-way and two-way relaying technique. New expressions for the end-to-end block error rate (BLER) for various nodes are derived in Section III-A, while expressions for the system throughput are provided in Section III-B. In addition, the asymptotic end-to-end BLER is analysed in Section III-C for all nodes in the presence of a high signal-to-noise ratio (SNR). In Section IV, we report the outcomes of our simulations, and in Section V, we draw a conclusion. The performance of the suggested method and its prospective applications in industrial automation and environment monitoring are both further clarified by this work.

The paper's notation is compiled in the following section. The $CN\left(0,\sigma^2\right)$ stands for the complex symmetric Gaussian random variable with variance $\sigma^2$ and mean zero. The $F_X\left(.\right)$ value represents a random variable's cumulative distribution function (CDF). $\mathrm{E}\left(.\right)$ represents the expectation operator. $\Pr\left(A/B\right)$ represents the conditional probability of event given, A and B.

## I. SYSTEM MODEL

In the proposed scenario, nodes $S_1$,$S_2$, and $D_2$ are paired together in a group to implement the NOMA scheme. These nodes share the same frequency and time resources within the group, while each group is allocated orthogonal resources from other groups. This allocation ensures efficient utilization of resources and supports simultaneous communication among the paired nodes. This scenario is in line with the proposed NOMA scheme and its application, as described in the referenced work.

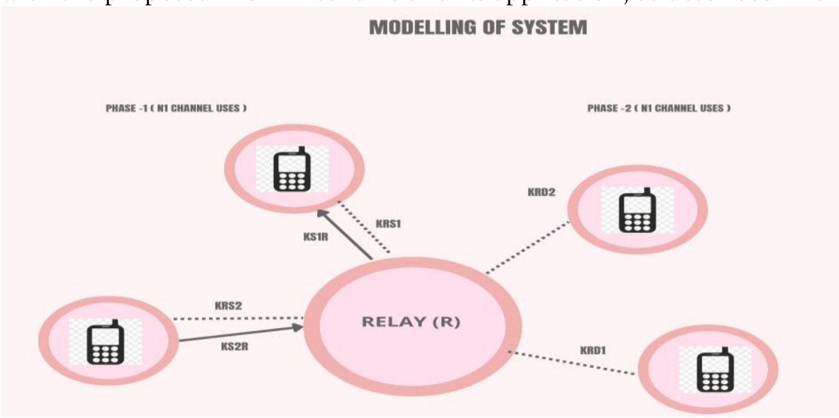


**Figure 1:** System model of NOMA Network with multiple relay connected with source node and destination node.

As can be seen in Figure 1, nodes $S_1$ and $S_2$ communicate with one another and transfer data to nodes $D_1$ and $D_2$ via a single DF relay R. Each node is assumed to have a single antenna and operate in half-duplex. Channel state information (CSI) is thought to be perfect at the receivers of the various links but simply statistical at the transmitters. No direct links are thought to exist between $S_1$ and $S_2$, or between $S_i$ and $D_i$ (i=1,2), either. It's possible for this to occur when there is either an excessive amount of ground to cover or when there are obstructions in the path. Let's say nodes $S_1$ and $D_2$ are in close proximity to the relay R, and nodes $S_2$ and $D_1$ are farther away. Distances between nodes R and U, $U \in \{S_1, S_2, D_1, D_2\}$, are mathematically expressed as $d(S_1, r) < d(S_2, r)$and $d(D_2, r) < d(D_1, r)$, respectively. The nodes exchange information during the two periods detailed below.

### A. Phase 1

First, two sources, S1 and S2, use channel n1 to send their symbols, x1 and x2, to a relay, R. This means that the signal at R can be written as

$$y_R = h_{S_1R}\sqrt{a_1P_S}x_1 + h_{S_2R}\sqrt{a_2P_S}x_2 + n_R \quad (1)$$

where the fading channel coefficient between $S_i$ and R is denoted by $K_{RU} \sim BM(0,\$), \$ = \frac{1}{(d(UR))^{v}}$, and the amount v represents the route loss exponent $\$^2_{S_1R} > \$^2_{S_2R}$ . It follows that .Assigning a percentage of the total available power to each of the two sources $S_1, S_2$, is denoted by the values $b_1P_S, b_2P_S$. When $S_1, S_2$, transmit at power-level $P_S$,, there is no need for a centralised power control mechanism (indicated by the setting $b_1 = b_2 = 1$ , but a centralised power controller is needed for the limitation $b_1 + b_2 \leq 1$ that limits the inter-cell interference [13]. The additive complex Gaussian noise at R is represented by the quantity $n_R \sim BM(0,\$^2_0)$. Since S_2 is superimposed on S_1, the relay ignores it as noise and decodes S_1. When R has decoded the first symbol, x_1, it subtracts the S_1 signal component from $X_R$ before moving on to decode the second symbol, $x_2$ of $S_2$.
If the relay perfectly decodes and cancels the interference of $X_1$, then the SINR for decoding $x_1$ at R and the SNR for decoding $x_2$ at R can be calculated as follows.

$$X_1^R = \frac{b_1\rho_S\beta_{S_1R}}{b_2\rho_S\beta_{S_2R}+1} \quad X_2^R = b\rho_S\beta_{S_2R} \quad (2)$$

where $\beta_{S_iR} = \left|K_{S_iR}\right|^2, i \in \{1,2\}$ and $\rho_S = \frac{P_S}{\sigma_0^2}$ . Since $K_{S_iR}$ follows an exponential distribution with rate parameter $\frac{1}{\$^2_{S_iR}}$, it follows that $\beta_{S_iR}$ also follows an exponential distribution.

**B. Phase 2**

Phase 2 entails the relay broadcasting the superposition of the decoded symbols $x_1$, $x_2$ to the nodes$D_1$, $D_2$ and the sources$S_1$, $S_1$ over $n_2$ channel uses. In this way, we may characterise the signal as it is received by node U:

$$X_{RU} = k_{RU}(\sqrt{a_1P_R}x_1 + \sqrt{a_2P_R}x_2) + n_u \quad (3)$$

The coefficient of the fading channel between R and node U is denoted by the expression $X_{RU} \sim BM(0,\$), \$^2_{UR} = \frac{1}{(d(UR))^{v}}$,. If $a_1 > a_2$ and $a_1 + a_2 \leq 1$, then a1 and a2 are the power factors for the x1 and x2 message symbols, respectively. The criterion $a1 > a_2$ [5] ensures that the NOMA downlink communication system distributes its transmission power fairly among its local and distant users. At node U, the complex additive Gaussian white noise is multiplied by the relay's transmit power, PR. When S1 and S2 subtract the signal components corresponding to their first phase broadcasts from the received signals $X_RS_1$ and $X_RS_2$, they are left with the symbols $X_2$ and $X_1$, respectively, which they may decode. This indicates that as long as the relay executes perfect SIC and correctly decodes $X_2$, $X_1$ the corresponding SNRs can be attained.

$$X_1^{S_2} = a_1\rho_R\beta_{RS_2}, yX_2^{S_1} = a_2\rho_R\beta_{RS_1} \quad (4)$$

where $\rho_R = \frac{P_S}{\$^2_0}$ . Node $D_1$ uses direct decoding to get the required message symbol $X_1$, while node $D_2$ employs SIC to get the required message signal $X_2$. The superposed signal corresponding to node $D_2$ is treated as interference. If perfect SIC has been applied at $D_2$, then the SINR for $X_1$ decoding at $D_i$ can be calculated as

$$X_1^{D_i} = \frac{(a_1\rho_R\beta_{RD_i})}{(a_2\rho_R\beta_{RD_i})+1}, x_2^{D_2} = a_2\rho_R\beta_{RD_2} \quad (5)$$

Following this part is a presentation of the typical BLER and resulting throughput for the aforementioned method.

## II. AVERAGE BLER AND THROUGHPUT ANALYSIS

**A. Statistics about the Typical BLER**

Take the two node pairs $D_1$, $S_2$, and $D_2$, $S_1$, and let $N_1$ and $N_2$ represent the number of bits of data that need to be transferred from $S_1$ and $S_2$, respectively. Any time the terminal U, where $U \in \{S_1, S_2, D_1, D_2\}$, incorrectly decodes the block corresponding to node $D_i$, i belongs to 1, 2, we will refer to this as the $\widetilde{U}$event. Let Permitted uses under licence are restricted to: University of Technology in Patna, India. Retrieved from IEEE Xplore on 2-17-2023 at 06:44:01 UTC. There are limits on this. The occurrence $\bar{\xi}_i^{\tilde{U}}$ is complemented by the action $\bar{\xi}_i^{\tilde{U}}$. The instantaneous BLER for a given SINR can be well approximated as using the fundamental result derived in [7], which is valid for block length $n \geq 100$

$$\tilde{\varepsilon} = Pr(\xi) \approx Q\left(\frac{n\,log_2(1+\gamma)-N)}{\sqrt{nV(\gamma)}}\right) \quad (6)$$

where Shannon capacity, channel dispersion coefficient, and the Gaussian Q-function are all denoted by the values $(x) = \frac{1}{\sqrt{2\pi}}\int_x^{\infty} e^{\frac{-t^2}{2}}\,dt$, $log_2(1+\gamma)$, $V(\gamma) = \left(1 - \frac{1}{(1+\gamma)^2}\right)(log_2\, e)^2$, respectively. Setting $\gamma = \gamma_1^R$as calculated in (2) and $N = N_2$, , $n = n_1$ in (6) yields the instantaneous probability of decoding $x_1$ in error at R, indicated as $\tilde{\varepsilon}_1^R = Pr(\xi_1^R)$. The instantaneous probability of decoding $x_2$ incorrectly at R, represented by $\tilde{\varepsilon}_k^D$, can be derived by substituting from (2) and, $n=n_i$ in (6) if R is able to decode and cancel the signal component corresponding to $x_1$ from $y_R$ in (1) without error. High levels of interference lead one to believe that complete SIC at R is required for successful decoding, as shown in studies such as [8], [10]. Therefore, the overall instantaneous BLER for $x_2$ decoding at R can be written as

$$\begin{aligned} Pr(\xi_2^R) &= Pr(\xi_2^R|\xi_1^R)\,Pr(\xi_1^R) + Pr(\xi_2^R|\bar{\xi}_1^R)\,Pr(\bar{\xi}_1^R) \Rightarrow \varepsilon_2^R = 1 \times \tilde{\varepsilon}_1^R + \tilde{\varepsilon}_2^R(1-\tilde{\varepsilon}_1^R) \\ &= \tilde{\varepsilon}_1^R + \tilde{\varepsilon}_2^R - \tilde{\varepsilon}_1^R\tilde{\varepsilon}_2^R \\ &\approx \tilde{\varepsilon}_1^R + \tilde{\varepsilon}_2^R \end{aligned} \quad (7)$$

where the final reduction in complexity is warranted by the fact that, as a result of the excellent reliability of 5G connectivity, the individual BLER terms $\tilde{\varepsilon}_1^R$, $\tilde{\varepsilon}_2^R$ are often quite tiny [1, 2]. Therefore, it is possible to proceed without considering the product term $\tilde{\varepsilon}_1^R\tilde{\varepsilon}_2^R$ [8]. Phase two involves R broadcasting the resultant signal to nodes $S_1$, $S_2$, and $D_1$, $D_2$. This signal is obtained by superposing the symbols decoded in phase one. After subtracting the contributions corresponding to their original symbols in the first phase, namely, $\sqrt{b_1 P_R}h_{RS_1}x_1$from $y_{RS_1}$and $\sqrt{b_2 P_R}h_{RS_2}x_2$ from $y_{RS_2}$, nodes $S_1$, $S_2$ decode their necessary symbols $x_2$, $x_1$, respectively. Therefore, if R correctly decodes the symbols $x_1$, $x_2$, the instantaneous probability of decoding the block $x_i$ at $S_i$ in error is indicated by $\tilde{\varepsilon}_j^{S_i} = Pr\left(\xi_j^{S_i}|\bar{\xi}_{1,2}^R\right)$. If the relay is able to successfully decode $x_1$ and $x_2$, the resulting quantity is written as $\bar{\xi}_{1,2}^R$. Substituting the SNRs $\gamma_j^{S_i}$from (4) and $N=N_i$, n=n_2 in (6) yields the formula. In addition, if the decoding at the relay is incorrect $\xi_{1,2}^R$then $Pr\left(\xi_j^{S_i}|\xi_{1,2}^R\right) = 1$.. With these definitions and data, we can calculate the end-to-end BLER at node S_i as

$$\begin{aligned} Pr\left(\xi_j^{S_i}\right) &= Pr\left(\xi_j^{S_i}|\xi_{1,2}^R\right)Pr(\xi_{1,2}^R) + Pr\left(\xi_j^{S_i}|\bar{\xi}_{1,2}^R\right)Pr(\bar{\xi}_{1,2}^R), \\ &\Rightarrow \varepsilon^{S_i} \approx 1 \times Pr(\xi_{1,2}^R) + \tilde{\varepsilon}_j^{S_i} \times Pr(\bar{\xi}_{1,2}^R), \\ &= 1 - \left(1 - \tilde{\varepsilon}_j^{S_i}\right) \times (1-\tilde{\varepsilon}_2^R) \times (1-\tilde{\varepsilon}_1^R) \approx \varepsilon_2^R + \tilde{\varepsilon}_j^{S_i}. \end{aligned} \quad (8)$$

The instantaneous BLER for decoding $x_2$ at R is calculated in Eq. (7); similarly, the BLER for decoding $x_1$ at $D_1$ can be calculated using the same method, yielding the expression.

$$\begin{aligned} &Pr(\xi_1^{D_1}) = Pr(\xi_1^{D_1}|\xi_1^R)\,Pr(\xi_1^R) + Pr(\xi_1^{D_1}|\bar{\xi}_1^R)\,Pr(\bar{\xi}_1^R), \\ &\Rightarrow \varepsilon^{D_i} \approx 1 \times \tilde{\varepsilon}_1^R + \tilde{\varepsilon}_1^{D_1}\left(1 - \tilde{\varepsilon}_j^{S_i}\right) \times (1-\tilde{\varepsilon}_1^R) \approx \tilde{\varepsilon}_1^R + \tilde{\varepsilon}_1^{D_i}. \end{aligned} \quad (9)$$

when we get ε˜ D1 1 by subbing in $N = N_1, n = n_2$ and $\gamma = \gamma_1^{D_1}$ from (5) in (6)'s primary BLER with FBL findings. The complete BLER at $D_2$ can be described using the same compact notation.

$$\varepsilon^{D_2} \approx \varepsilon_2^R + \tilde{\varepsilon}_1^{D_2} + \tilde{\varepsilon}_2^{D_2} \quad (10)$$

where $\varepsilon_2^R$ is given in (7) and can be achieved by exchanging γ D2 k from (5) together with $N = N_k$and $n = n_2$, in (6). Finally, the typical terminal end-to-end BLER $S_i$, $D_i$, can be obtained as

$$E(\varepsilon^{S_i}) \approx E(\varepsilon_2^R) + E\left(\tilde{\varepsilon}_j^{S_i}\right) \quad (11)$$

$$E(\varepsilon^{D_1}) \approx E(\tilde{\varepsilon}_1^R) + E\left(\tilde{\varepsilon}_1^{D_1}\right) \quad (12)$$

$$E(\varepsilon^{D_2}) \approx E(\varepsilon_2^R) + E\left(\tilde{\varepsilon}_1^{D_2}\right) + E\left(\tilde{\varepsilon}_2^{D_2}\right) \quad (13)$$

To simplify the instantaneous BLER, we can use the following approximation, which is based on [14], since a direct calculation of the predicted value of the BLER expression in (6) is mathematically intractable.

$$\tilde{\varepsilon}_i^{\tilde{U}} \approx \begin{cases} 1, \gamma_i^{\tilde{U}} \leq \zeta_i^{\tilde{U}}, \\ \frac{1}{2} - T_i^{\tilde{U}}\sqrt{n}\left(\gamma_i^{\tilde{U}} - \psi_i^{\tilde{U}}\right), \zeta_i^{\tilde{U}} < \gamma_i^{\tilde{U}} < \Delta_i^{\tilde{U}}, \\ 0, \gamma_i^{\tilde{U}} \geq \Delta_i^{\tilde{U}}, \end{cases} \quad (14)$$

Where $\tau_i^{\tilde{U}} = \left(2\pi\left(2^{\frac{2N_i}{n}} - 1\right)\right)^{\frac{-1}{2}}$, $\psi_i^{\tilde{U}} = 2^{\frac{N_i}{n}} - 1$, $\zeta_i^{\tilde{U}} = \psi_i^{\tilde{U}} - \frac{1}{2\tau_i^{\tilde{U}}\sqrt{n}}$, $\Delta_i^{\tilde{U}} = \psi_i^{\tilde{U}} + \frac{1}{2\tau_i^{\tilde{U}}\sqrt{n}}$. Using the preceding result, the likely value of $\tilde{\varepsilon}_i^{\tilde{U}}$ can be well approximated as

$$E\left(\tilde{\varepsilon}_i^{\tilde{U}}\right) \approx T_i^{\tilde{U}}\sqrt{n}\int_{\zeta_i^{\tilde{U}}}^{\Delta_i^{\tilde{U}}} F_{\gamma_i^{\tilde{U}}}(x)dx \quad (15)$$

where $F_{\gamma_i^{\tilde{U}}}(x)$ denotes the CDF of $\gamma_i^{\tilde{U}}$ . To assess the analytical expressions for the average BLERs at different terminals, we shall use the preceding expression in (15).

**Scenario 1.** Given that $x_1$ has been correctly decoded at R, the average BLER for decoding $x_2$ is

$$E(\tilde{\varepsilon}_2^R) \approx 1 - \frac{T_2^R\sqrt{n_1}\rho_S}{\phi_3}\left\{E_i\left(-\frac{\phi_1(1+\phi_2\Delta_1^R)}{\phi_2\rho_S}\right) - E_i\left(-\frac{\phi_1(1+\phi_2\zeta_1^R)}{\phi_2\rho_S}\right)\right\} \quad (16)$$

$$E\left(\tilde{\varepsilon}_1^{D_2}\right) \approx 1 - \frac{T_2^R\sqrt{n_1}\rho_S}{\phi_3}\left\{e^{-\frac{\phi_3\zeta_2^R}{\rho_S}} - e^{-\frac{\phi_3\Delta_2^R}{\rho_S}}\right\} \quad (17)$$

where $\Delta_1^R < \frac{a_1}{a_2}$. The quantity $Ei(-x) = -\int_x^\infty \frac{exp(-t)}{t}dt$, the integral of the exponential function [15] and $\phi_1 = \frac{1}{a_1\sigma_{S_1R}^2}$, $\phi_2 = \frac{a_2\sigma_{S_2R}^2}{a_1\sigma_{S_1R}^2}$, $\phi_3 = \frac{1}{a_2\sigma_{S_2R}^2}$.

**Proof.** A comprehensive demonstration may be found in Section I of the technical report of this paper, which can be found in [16]. When the aforementioned formulae are substituted into equation (7) in place of $E(\tilde{\varepsilon}_1^R)$ ) and $E(\tilde{\varepsilon}_2^R)$, which are obtained from equations (16) and (17), respectively, the result is $E(\varepsilon_2^R)$.

**Scenario 2.** The expressions for the average BLERs $E\left(\tilde{\varepsilon}_2^{D_2}\right)$, $E\left(\tilde{\varepsilon}_j^{S_i}\right)$ where $j \in \{1,2\}, j \neq i$ are given below. The expressions for the average BLERs relate to the second phase of communication, which is designated by the notation $E\left(\tilde{\varepsilon}_1^{D_i}\right), i \in \{1,2\}$. The expression for the average BLERs is given in (18).

$$E\left(\tilde{\varepsilon}_2^{D_2}\right) \approx 1 - \frac{T_2^{D_2}\sqrt{n_2}\rho_R}{\phi_4}\left\{e^{-\frac{\phi_4\zeta_2^{D_2}}{\rho_R}} - e^{-\frac{\phi_4\Delta_2^{D_2}}{\rho_R}}\right\} \quad (19)$$

$$E\left(\tilde{\varepsilon}_i^{S_i}\right) \approx 1 - \frac{T_2^{D_2}\sqrt{n_2}\rho_R}{\phi_4}\left\{e^{-\frac{\phi_4\zeta_2^{D_2}}{\rho_R}} - e^{-\frac{\phi_4\Delta_2^{D_2}}{\rho_R}}\right\} \quad (20)$$

Where $\phi_4 = \frac{1}{b_2\sigma_{RD_2}^2}$ and $\tilde{\phi}_{ij} = \frac{1}{b_j\sigma_{RS_i}^2}$.

**Proof.** Section II of this paper's technical report [16] provides a comprehensive verification of the central thesis. Using the average BLER expressions $(\tilde{\varepsilon}_1^R)$,$E(\varepsilon_2^R)$, $E\left(\tilde{\varepsilon}_1^{D_i}\right)$, $E\left(\tilde{\varepsilon}_j^{S_i}\right)$, and $E\left(\tilde{\varepsilon}_j^{S_i}\right)$ determined above, one can solve for the end-to-end average BLERs $E(\varepsilon^{S_i})$, $E(\varepsilon^{D_i})$ at each of the nodes $S_1$, $S_2$, $D_1$, $D_2$.

**B. An Overview of the System's Typical Throughput**

The typical system throughput is represented by [9].

$$r_{th} = \sum_U r_U T_U\left(1 - E(\varepsilon^U)\right) \quad (21)$$

for each rU = NU Where $U \in \{S_1, S_2, D_1, D_2\}$, n˜U represents the rate of data transmission to node U, where $N_U$is the number of data bits transmitted and $\tilde{n}_U \geq 100$ is the number of channels uses. The end-to-end average BLER at node U is denoted by the expression E(U), and the proportion of the entire communication interval allotted for transmission to node U is denoted by the expression $T_U = \frac{\tilde{n}_U}{\tilde{n}}$, where $\tilde{n}_U = \sum_U \tilde{n}_U$signifies the sum total of channel uses employed for transmission to all nodes $S_1$, $S_2$, $D_1$, and $D_2$, respectively. Our calculations show that $\tilde{n}_U = \tilde{n} = n_1 + n_2 \geq 200$.is the optimal number of nodes for the proposed NOMA-based two-phase combined two-way and one-way relaying mechanism. However, since end-to-end communication in an OMA-based system occurs in four stages with a minimum of 100 channel usage per phase, it is clear that $\tilde{n}_U \geq 200$ and $\tilde{n} \geq 400$,. To be more specific, during the first and second phases, $S_1$ and $S_2$ send SNR _Sand the information symbols $x_1$ and $x_2$ to R, respectively, using $m_1 \geq 100$ and $m_2 \geq 100$ channel uses, respectively. Each phase's decoded information symbols, $x_1$ and $x_2$, are transmitted from R using the $m_3 \geq 100$ and $m_4 \geq 100$ channels with a transmit SNR of _R to destinations $D_1$, $S_2$, and $D_2$, $S_2$, respectively.

**C. Analysis of High Signal-to-Noise Ratio (BLER)**

Additional information about the system's performance can be gleaned from the expressions presented in this part, which describe the end-to-end BLER at high signal-to-noise ratio (SNR). Denote by $E\left(\tilde{\varepsilon}_j^U\right)$ the asymptotic value of the BLER at high SNR.

First postulate: when the signal-to-noise ratio (SNR) is high, the expression for the BLER from node U to the end can be estimated as

$$E(\tilde{\varepsilon}^U) \approx 1 - \frac{T_1^R \sqrt{n_1}}{\phi_2} ln\left(\frac{1+\phi_2 \Delta_1^R}{1+\phi_2 \zeta_1^R}\right) \quad (22)$$

**Proof.** Section III of the technical report of this publication [16] presents the proof in detail.

Since the uplink signal from $S_1$ is subject to the most interference, this is intuitively to be expected. As a result, all the nodes' decoding will be off if there's a problem with decoding $x_1$ at R. As can be shown from (22), the average BLER for decoding $x_1$ at R dominates the end-to-end average BLER at all nodes when the SNR is large.

## III. SIMULATION RESULTS

The performance of the proposed system is then demonstrated by simulation results, which are also used to verify the accuracy of the analytical results. The power factors of the source and the relay have been set to a_1=0.8, a_2=0.2, and b_1=0.8, b_2=0.2, respectively, in accordance with the values specified in works like [5], [8]. $P_R = P_S$means that the combined transmit powers of the source and relay are equal. We've decided that $d(S_1, R) = d(R, D_2) = 0.5m$ and $d(S_2, R) = d(R, D_1) = 1m$ is the optimal distance between a relay and a user node. Exponent v = 3 has been chosen for path loss. The approximation for the BLER in (6) is guaranteed to be true because the amount of user bits $N_1 = N_2 = 30$ and the number of channel uses or block lengths evaluated are $n_1$=$n_2$=100. End-to-end bit error rate (BLER) vs signal-to-noise ratio (SNR) at nodes $S_1$ and $S_2$ is displayed in Fig. 2(a) and Fig. 2(b), respectively. The analytical expressions in (11), (12), and (13) developed in subsection III-A show a high degree of agreement with the simulated results. At SNRs greater than 30 dB, the asymptotic floor computed in (22) is found to be in good agreement with the simulated end-to-end BLERs. The proposed NOMA-based FBL s cheme's average system throughput computed using (21) versus signal-to-noise ratio (SNR) is shown in Fig. 2(c) for two scenarios of user data bits, namely $N_1$=N2=100 and 50. In the suggested system, $n_1$ = $n_2$ = 100 represents the equality between the total number of channel usage in the first and second phases. Therefore, with total source and relay transmit SNR $\rho_S + \rho_R$, one obtains $\tilde{n}_U = \sum_U \tilde{n}_U$and $T_U = 1$ for the NOMA-based system, as indicated in section III-B. Figure 2(c) also includes data on the efficiency of an OMA-based FBL system, as detailed in subsection III-B. Each transmission phase will use 100 channel allocations ($m_1, m_2, m_3, m_4 = 100$). Therefore, with a total source and relay SNR of $2\rho_S + 2\rho_R$, we $\tilde{n}_U = 200, \tilde{n} = 400$ and $T_U = \frac{1}{2}$ for the OMA-based system. As can be seen in the graphic, the suggested NOMA scheme significantly outperforms its OMA equivalent.

$$E\left(\tilde{\varepsilon}_1^{D_i}\right) \approx 1 - \frac{\tau_1^{D_i}\sqrt{n_2}\, e^{\frac{1}{b_2\rho_R\sigma_{RD_i}^2}}}{b_2}\left[\frac{b_1}{b_2\rho_R\sigma_{RD_i}^2}\left\{E_i\left(-\frac{b_1}{b_2\rho_R\sigma_{RD_i}^2\left(b_1-\zeta_1^{D_i}b_2\right)}\right) - E_i\left(-\frac{b_1}{b_2\rho_R\sigma_{RD_i}^2\left(b_1-\Delta_1^{D_i}b_2\right)}\right)\right\} + \left\{\left(b_1-\zeta_1^{D_i}b_2\right)e^{\left(\frac{-b_1}{b_2\rho_R\sigma_{RD_i}^2\left(b_1-\zeta_1^{D_i}b_2\right)}\right)} - \left(b_1-\Delta_1^{D_i}b_2\right)e^{\left(\frac{-b_1}{b_2\rho_R\sigma_{RD_i}^2\left(b_1-\Delta_1^{D_i}b_2\right)}\right)}\right\}\right], \Delta_i^{D_i} < \frac{b_1}{b_2}.$$
(18)

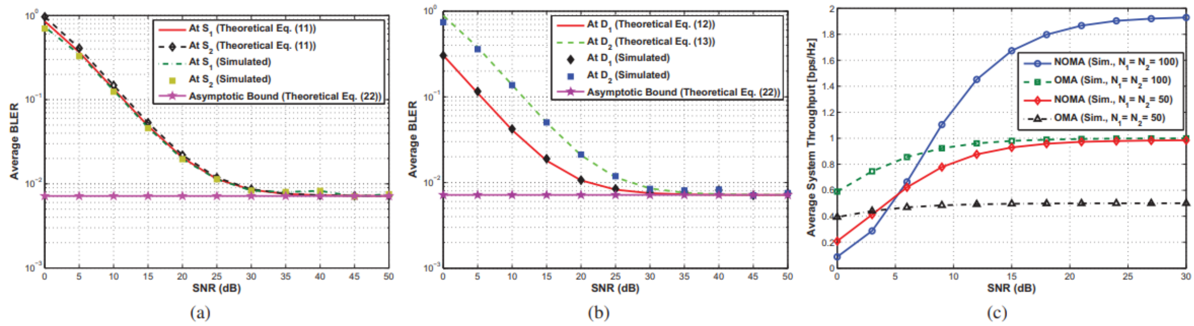


**Figure 1:** Average BLER for NOMA Network at different SNR value (a) at S1; S2. (b) at D1; D2. (c) Average System Throughput for NOMA Network at different SNR value.

The figure shows that the proposed NOMA scheme works far better than its OMA counterpart over a large range of signal-to-noise ratios (SNRs), with the exception of low SNRs, when NOMA performs poorly due to error propagation in SIC. In NOMA, the communication process occurs in multiple phases. During the first and second phases, the total power available for transmission is limited to a certain budget, represented by of $\rho_S$ and $\rho_R$ . This means that the power allocated for each symbol in NOMA is constrained by this budget. On the other hand, in the conventional OMA system, the power allocation for each symbol is determined based on achieving the maximum possible Signal-to-Noise Ratio (SNR) for transmission. In other words, OMA uses the highest achievable power level, without considering any specific power budget restrictions. The key point here is that NOMA can achieve higher throughput, which refers to the amount of data that can be transmitted successfully, while still operating within a limited power budget. By carefully managing the power allocation across different phases of the communication process, NOMA can make more efficient use of the available power resources, leading to increased throughput compared to OMA. Overall, the main advantage of NOMA is its ability to boost the amount of data transmitted while operating within a restricted power budget, making it an attractive option for improving communication efficiency.

## IV. CONCLUSION

This paper presents an energy-efficient communication strategy integrating finite block length (FBL) NOMA with hybrid one-way and two-way relaying, aimed at enhancing performance in smart and sustainable environments. Closed-form expressions for average BLER, throughput, and high-SNR behavior were derived and validated through simulation, demonstrating the proposed scheme's reliability and efficiency. Compared to traditional FBL-OMA systems, the NOMA-based approach offers significant performance gains, particularly with optimized power allocation. While this paper establishes a solid foundation, future work may focus on dynamic power allocation and resource optimization to further improve energy efficiency and system sustainability in evolving smart communication networks.

## REFERENCES

[1] G. Durisi, T. Koch, and P. Popovski, “Toward massive, ultrareliable, and low-latency wireless communication with short packets,” Proceedings of the IEEE, vol. 104, no. 9, pp. 1711–1726, 2016.
[2] H. Chen, R. Abbas, P. Cheng, M. Shirvanimoghaddam, W. Hardjawana, W. Bao, Y. Li, and B. Vucetic, “Ultra-reliable low latency cellular networks: Use cases, challenges and approaches,” IEEE Communications Magazine, vol. 56, no. 12, pp. 119–125, 2018.

[3] Y. Liu, Z. Qin, M. Elkashlan, Z. Ding, A. Nallanathan, and L. Hanzo, "Non-orthogonal multiple access for 5G and beyond," Proceedings of the IEEE, vol. 105, no. 12, pp. 2347–2381, 2017.
[4] D. Wan, M. Wen, F. Ji, H. Yu, and F. Chen, "Non-orthogonal multiple access for cooperative communications: Challenges, opportunities, and trends," IEEE Wireless Communications, vol. 25, no. 2, pp. 109–117, 2018.
[5] X. Yue, Y. Liu, S. Kang, A. Nallanathan, and Y. Chen, "Modeling and analysis of two-way relay non-orthogonal multiple access systems," IEEE Transactions on Communications, vol. 66, no. 9, pp. 3784–3796, 2018.
[6] C. E. Shannon, "A mathematical theory of communication," ACM SIGMOBILE mobile computing and communications review, vol. 5, no. 1, pp. 3–55, 2001.
[7] Y. Polyanskiy, H. V. Poor, and S. Verdu, "Channel coding rate in the ´ finite blocklength regime," IEEE Transactions on Information Theory, vol. 56, no. 5, pp. 2307–2359, 2010.
[8] Y. Yu, H. Chen, Y. Li, Z. Ding, and B. Vucetic, "On the performance of non-orthogonal multiple access in short-packet communications," IEEE Communications Letters, vol. 22, no. 3, pp. 590–593, 2018.
[9] X. Sun, S. Yan, N. Yang, Z. Ding, C. Shen, and Z. Zhong, "Short-packet downlink transmission with non-orthogonal multiple access," IEEE Transactions on Wireless Communications, vol. 17, no. 7, pp. 4550–4564, 2018.
[10] J. Zheng, Q. Zhang, and J. Qin, "Average block error rate of downlink NOMA short-packet communication systems in Nakagami-m fading channels," IEEE Communications Letters, 2019.
[11] X. Lai, Q. Zhang, and J. Qin, "Cooperative NOMA short-packet communications in flat Rayleigh fading channels," IEEE Transactions on Vehicular Technology, 2019.
[12] Y. Gu, H. Chen, Y. Li, L. Song, and B. Vucetic, "Short-packet two-way amplify-and-forward relaying," IEEE Signal Processing Letters, vol. 25, no. 2, pp. 263–267, 2018.
[13] Z. Yang, Z. Ding, P. Fan, and N. Al-Dhahir, "A general power allocation scheme to guarantee quality of service in downlink and uplink NOMA systems," IEEE Transactions on Wireless Communications, vol. 15, no. 11, pp. 7244–7257, 2016.
[14] B. Makki, T. Svensson, and M. Zorzi, "Finite block-length analysis of the incremental redundancy HARQ," IEEE Wireless Communications Letters, vol. 3, no. 5, pp. 529–532, 2014.
[15] I. S. Gradshteyn and I. M. Ryzhik, Table of integrals, series, and products. Academic press, 2014.
[16]. Shankar R., Kumar I., Mishra R.K. (2019). Outage probability analysis of MIMO-OSTBC relaying network over Nakagami-m fading channel conditions, Traitement du Signal, Vol. 36, No. 1, pp. 59-64. https://doi.org/10.18280/ts.360108.
[17]. Kumar, I., Mishra, M.K., Mishra, R.K. (2021). Performance analysis of NOMA downlink for next-generation 5G network with statistical channel state information. Ingénierie des Systèmes d'Information, Vol. 26, No. 4, pp. 417-423. https://doi.org/10.18280/isi.260410
[18]. Shankar, R., Kumar, I., Mishra, R.K. (2019). Pairwise error probability analysis of dual hop relaying network over time selective Nakagami-m fading channel with imperfect CSI and node mobility. Traitement du Signal, Vol. 36, No. 3, pp. 281-295. https://doi.org/10.18280/ts.360312.
[19]. Kumar I, Kumar A, Kumar Mishra R. Performance analysis of cooperative NOMA system for defense application with relay selection in a hostile environment. The Journal of Defense Modeling and Simulation. 2022;0(0). doi:10.1177/15485129221079721.
[20]. Ashish, I. Kumar and R. K. Mishra, "Performance Analysis For Wireless Non-Orthogonal Multiple Access Downlink Systems," 2020 International Conference on Emerging Frontiers in Electrical and Electronic Technologies (ICEFEET), Patna, India, 2020, pp. 1-6, doi: 10.1109/ICEFEET49149.2020.9186987.
[21]. A. Agarwal and A. K. Jagannatham, "Technical Report: NOMA-based joint one-way and two-way relaying aided finite blocklength communication." IIT Kanpur, Kanpur, India, Technical Report, 2020. [Online]. Available: http://www.iitk.ac